Waste heat to power conversion by means of thermomagnetic hydrodynamic energy harvester

Alessandro Chiolerio [1], Erik Garofalo [1, 2], Fabio Mattiussi [1,2†], Marco Crepaldi [3], Giuseppe Fortunato [1,4††] and Michele Iovieno [4]*

[1]Istituto Italiano di Tecnologia, Center for Sustainable Future Technologies, Via Livorno 30, 10144 Torino, Italy;

[2]Politecnico di Torino, Department of Electronics, Corso Duca degli Abruzzi 24, 10129 Torino, Italy;

[3]Istituto Italiano di Tecnologia, Electronic Design Laboratory, Via Enrico Melen 83, 16152 Genova, Italy;

[4]Politecnico di Torino, Department of Mechanical and Aerospace Engineering, Corso Duca degli Abruzzi 24, 10129 Torino, Italy;

† Now at SPEA S.p.A., Via Torino, 16 10088 Volpiano (TO) – Italy;

†† Now at Strathclyde University, 16 Richmond St, Glasgow G1 1XQ, United Kingdom.

Corresponding Author

alessandro.chiolerio@iit.it

Abstract

The first closed-loop thermomagnetic hydrodynamic energy harvester, based on thermomagnetic advection and exploiting a commercial ferrofluid, is described. The lab-scale prototype has a toroidal geometry adopted from the well-known tokamak inertial machines. Peltier modules are used to control the thermal gradient that is harvested and converted directly to electric energy, while permanent magnets trigger the advection. Temperature sensors are installed along the toroidal walls (thermistors) and are placed in contact with the rotating fluid (thermocouples). To extract and ensure the electrical energy output, the structure is wrapped-up with coils and connected to an impedance meter and pico-amperometer. Two coil configurations (purely poloidal and mixed poloidal/toroidal windings) are tested, in a heterogeneous two-phase flow from the combination of water carrier and ferrofluid packets, reaching a maximum extracted electrical power per unit of temperature difference of 10.4 μW/°C, that is approximately 20% of the ideal Carnot efficiency of a thermal machine working on the same temperature drop. Numerical analysis of the system has been performed developing a Fortran™ code in a Eulerian framework, using a mixed Fourier-Galerkin/finite difference spatial discretization.

List of Acronyms

Brayton Cycle (BC)

Carbon Dioxide Trans-Critical Cycle (CDTCC)

Central Processing Unit (CPU)

Colloidal EneRgEtic System (CERES)

Ferrofluid (FF)

Field Programmable Gate Array (FPGA)

Fused Deposition Modelling (FDM)

Graphics Processing Unit (GPU)

Industrial Waste Heat (IWH)

Kalina Cycle (KC)

Micro-Electro-Mechanical Systems (MEMS)

Organic Rankine Cycle (ORC)

Peltier Array Controller (PAC)

PolyLactic Acid (PLA)

Pulse Width Modulation (PWM)

Stirling Cycle (SC)

Thermoelectric (TE)

ThermOmagnetic hydRODYNAmic energy harvester (TORODYNA)

Waste Heat to Power (WHP)

Waste Heat Recovery (WHR)

Introduction

Energy utilization together with sustainable processes and care for the environment are now under the spotlight; transforming energy for the benefit and development of human society must take into account the non-unitary efficiency of any process, and the consequent distributed production of waste heat, playing therefore a role in global warming, whose effect has been measured to impact severely our economy [1]. To highlight the critical aspect of energy issues, we may recall that the world energy consumption in 2040 is expected to surpass 200,000 TWh/year, leading to heat wasted into the environment of approximately 120,000 TWh/year. Its trend has been monotonically increasing since the beginning of the first industrial era, in 1840 [2]. The value of this incredible amount of energy, if we suppose a conversion and injection to the electric grid with an average efficiency around 30 %, is close to 50 billion €/y. Recent analysis about the U.S. market highlights a forecast, depending on policy scenario, that could produce between 3 and 4 EJ of green energy using all available wastes [3]. A greatly valuable approach to tackle this problem is to capture and reuse the waste heat, providing an attractive opportunity for an emission-free and cost effective energy resource [4], though the cost per kW of such solutions might be quite high and must be evaluated using sophisticated models to quantify the IWH potential [5]. Energy harvesting can be defined as the process *wherein the sources such as mechanical load, vibrations, temperature gradients, heat, light, salinity gradients, wind, etc., are scavenged and converted to obtain relatively small levels of power in the nW-mW range* [6]. *In particular, WHP is the process of converting the heat discarded by an existing process and using that heat to generate electricity via thermodynamic cycles,* thermoelectric, triboelectric and pyroelectric devices, or thermomagnetic hydrodynamic systems [7]. Improving overall energy efficiency, together with the use of renewables and the increase of

energy access to populations, as listed by UN “Sustainable energy for all” policy, is also compatible with the global warming limit of 2 °C [8].

Over the years several approaches to WHR have been developed. Thermodynamic systems based on BC, SC, KC, CDTCC, ORC are widely employed in the industrial sector. As examples, BC has been used in a WHR system including heat exchangers coupled to a turbocharger which converts waste heat into enthalpy and an electric generator that converts it into electromagnetic energy, improving the fuel efficiency by 10 % [9]. In the cement industry, KC is implemented generating ammonia-water vapor harvesting low-grade heat, then it is expanded in a turbine, condensed in regenerative heat exchangers, diluted and fed into a low-pressure condenser and finally injected into the high-pressure condenser before reaching again the vapor generators [10].

Adsorption refrigeration, often used with solar collectors other than waste heat, provides direct heat re-use [11]. TE materials [12], on the other hand, feature conversion of heat into electric energy, but are quite far from the ideal Carnot cycle [13]. At the very small scale, in terms of volumes (< 10 cm^3) and masses (< 1 kg), several solutions have been brought to reasonable efficiencies: MEMS enabling micro-combustors, micro-turbines, micro-fuel cells, often combined with thermoelectric modules, are an example [14].

In table 1 the main commercially-exploited systems for WHR are compared [15-19].

LT=Low Temperature *HT=High Temperature*	*BC*	*ORC*	*KC*	*TE*
η @ LT (T_{Hot} < 250 °C) [%]	17	6.5	13	4
η @ HT (250 < T_{Hot} < 450 °C) [%]	21	13	18	6
Typical installed power per plant [MW]	7.8	0.35	0.4	0.012
Cost per kW [k€/kW]	1.8	0.065	2.5	3.2

Table 1: Comparison between the main commercially-exploited systems for WHR.

Other more exotic physics could be used, for example the Nernst transverse thermoelectric effect (an electrical field that appears out of the plane formed by a thermal gradient and perpendicular magnetic field), but involving very peculiar and dangerous materials, such as URu_2Si_2 heavy Fermion superconductor [20]. Another interesting, green approach, has been that of using cellulosic membranes, infiltrated with electrolytes and submitted to a thermal gradient parallel to the fibers, to exploit differential ionic conductivity and generate a thermally induced electromotive force as high as 24 mV/°C and a resulting power of 5.76 μW / °C [21]. This approach belongs to the liquid state electrochemical systems, discussed in a broader context and reviewed in detail elsewhere [22].

The economic feasibility for WHP declines as the amount and quality of the heat decreases [23]. For these reasons, a TORODYNA energy harvester was developed and characterized, an apparatus that belongs to the so called CERES family, where a colloid is exploited either to store or to harvest energy from a specific gradient [24]. The idea behind this work derives from the awareness of unprecedented thermophysical potential of FFs [25]. FFs are suspensions of magnetic nanoparticles dispersed in non-magnetic liquids, categorized as a class of functional fluids whose flow and energy transport processes can be influenced and controlled by adjusting the strength and orientation of an external magnetic field [26], although, in experiments and theoretical investigations it is often found that the magnetically induced effects are strongly coupled with gravitationally driven phenomena [27]. Starting from the studies and simulations of Yang et al. [26], results exploited the thermomagnetic advection effect (thermal gradient parallel to external magnetic field) of a FF contained in a closed loop geometry.

Typically, the principal aim is a more efficient thermal dissipation, in particular in those applications such as laptops and high thermal density CPUs, where a passive system is more reliable and less impacting on the batteries power availability [28]. High performance commercial devices (CPUs and GPUs) already went above the thermal energy density of nuclear power reactors (200 Wcm^{-2}) and rocket nozzles (1 $kWcm^{-2}$) and are approaching that of the Sun surface (10 $kWcm^{-2}$) [29, 30]. Some existing FF-based solutions include an active pumping system that adsorbs energy from an external source. However, these devices are not optimized for energy production only, but are conceived to dissipate heat and to recover a tiny portion of the energy available as kinetic energy [31]. The energy output is typically low, 20 μV across a 1,000 turn copper-wire of 130 μm diameter (1,300 Ω/km leading to around 50 Ω) corresponding to 80 fW [32]. Another interesting application is that of electromagnetic induction by FF in an

oscillating heat pipe, a device that operates harvesting the thermal gradient between a heat source and a heat sink using a meandering closed-loop tube filled with FF, magnetized by permanent magnets and forced to move across an extraction coil [33]. For this application, the required thermal gradient must be high enough to induce a phase transition in the FF solvent, creating vapor that propels the fluid in the circuit, with a resulting figure of merit of 10 pW/°C, one million times lower than the device described in the present report. Steady oscillations are established with rather high thermal power, above 70W, thus preventing applications in wearable/portable devices/appliances [34]. Thermomagnetic cycles on Gd rotors have been shown to convert waste heat starting from 2 °C of ΔT with the output of 52.5 μW /Kcm^3 [35]. Another interesting device, again operating against 20 °C of ΔT, was fabricated to exploit thermomagnetic effects (change of magnetization in a solid state material, when subjected to a thermal cycle) and induce currents in a coil, with a remarkable output of 1 mW under certain conditions, with the drawback of requiring exotic materials, like La-Fe-Co-Si [36]. Against a 40 °C of ΔT the technology of thermo-osmotic waste heat recovery promises interesting power densities in the order of 1 Wm^{-2} [37]. Much lower power could be extracted (550 fW/°C) if, instead of using special membranes, conical holes are drilled to separate the two reservoirs [38]. Other relevant examples are the works of Zhou et al. [39] in which a thermo-magnetic based device exploits the magnetic fluid motion to drive a mechanical rotor and of Yamaguchi et al. [40], investigating the characteristic of a thermo-magnetic driven motor exploiting a magnetic fluid. In both cases the devices are not able to harvest electrical energy.

Figure 1 presents an overview of the application ranges of some of the above mentioned technologies which can be used in the whole range of low-grade waste heat. The main solutions are put in correlation in function of the ΔT available and grouped according to the three main

application fields, namely portable, domestic and industrial. It is clear that thermomagnetic hydrodynamic systems such as TORODYNA are suitable in the ΔT range from 1 to 100 °C especially for portable and domestic applications.

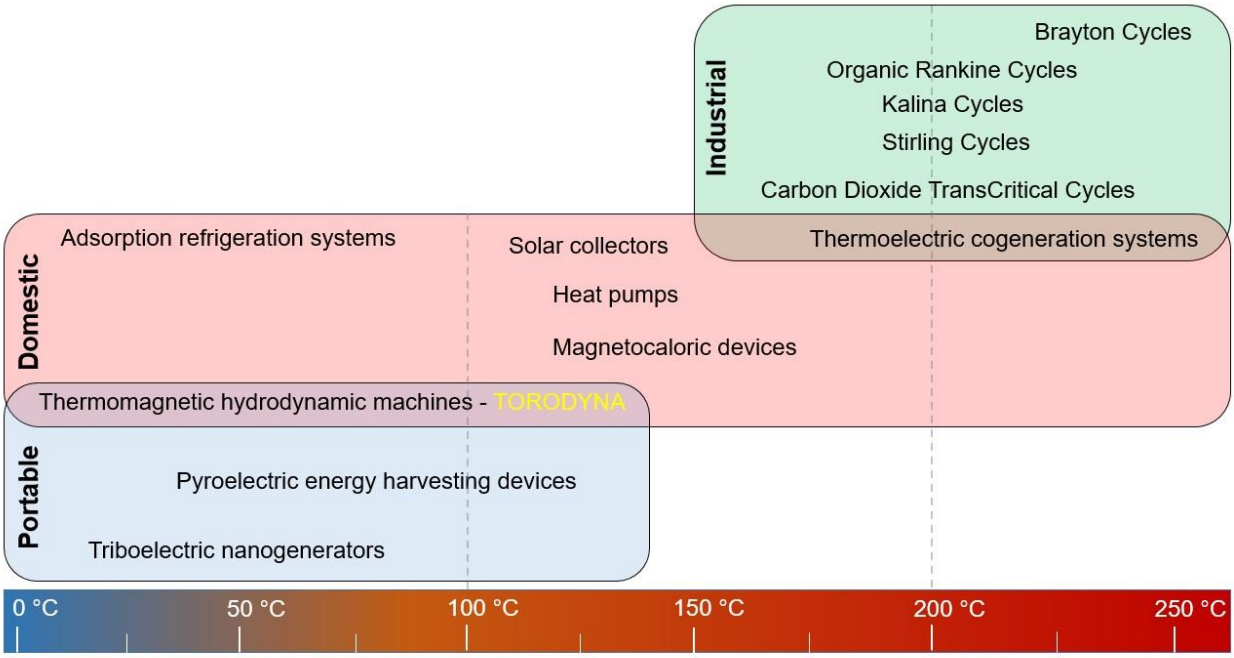

Figure 1: Overview of the main existing technologies for WHR/WHP, grouped according to the main application fields and as a function of the available ΔT.

The TORODYNA: novelty and layout

The TORODYNA concept we propose is able to provide an output with the lowest ΔT ever reported, as low as 1.25 °C, and the highest output per unit of temperature difference in the LT range, is robust, low-cost and based on non-toxic materials. TORODYNA features: 1) a purely liquid aggregation state of the active medium that does not require high thermal inputs since it does not undergo phase transition; 2) the container features a toroidal shape, a choice that allows to have a closed loop for the active medium and to easily put in thermal contact the container

walls with hot and cold reservoirs; 3) thermomagnetic advection, a physical effect that is observed when FFs are submitted to a thermal gradient parallel to a magnetic field, which induces a motion of the FF in transverse direction; 4) the Ludwig-Sorèt effect, which induces density gradients in the magnetic nanoparticles that influence the remanent magnetization of the FF; 5) the stabilization of magnetic particle density waves known as "Hopfions" (Figure 2a), whose layout is that of knots twisted around the toroidal cycle (*i* coordinate system) *p* times and twisted around the poloidal cycle (*j* coordinate system) *q* times; 6) magnetic induction as extraction principle. Combining thermal magnetic advection and Ludwig-Sorèt effect to induce density waves (Hopfions [41]) moving in a closed loop (topology) is the core of the TORODYNA technology, enabling operations with extremely small thermal gradients, as low as 1.25 °C, with unprecedented conversion efficiencies, million times higher than existing induction-based technologies. It is noteworthy to state that, using induction coils and a homogeneous composition of a high magnetic permeability core moving inside the coils, no electromotive force will be measured when the magnetic flux variation is negligible with respect to the coil volume. Therefore in a toroidal container filled with an homogeneous magnetic fluid set in motion, we will measure no electromotive force on poloidal windings. Density waves appear and move in the structure and self-organize into clusters from whose movement it is possible to extract electromagnetic energy. Using a curved geometry, instead of a flat one, and imagining to close the loop offering the FF a circular trajectory useful for electromagnetic conversion as later described, the torus was selected as optimal choice. The torus is a void container, thermally conductive and magnetically transparent, fabricated using carbon filled PLA filament and 3d printed with FDM technology, featuring an internal volume of 1 L (Figure 2b). The thermal gradient is set across the container walls, as the magnetic field does, and resulting

density waves accomplish integer twists along the toroidal and poloidal axes and generate a stable helical flow of magnetically charged particles, similar to the helical plasma flow in nuclear fusion reactors. The condition to achieve such flow is the collinearity between thermal gradient controlled by Peltier cells and magnetic field lines, obtained by AlNiCo permanent magnets. The thermal gradient is established by the Peltier cells controlled by a PAC electronic system, capable of PWM control of the cells and at the same time capable of measuring the temperature from the thermocouples/thermistors with commercial I2C read-out components. The total number of Peltier cells was selected by design: the converter was dimensioned for a total liquid volume of 1 L, hence its inner and outer radii were calculated after fixing the container width. Fabrication constraints given by the 3D printing of the container, about wall thickness, led us to choose the smallest Peltier cells available in order to create a mosaic of sections around the torus surface to change the thermal gradient and to set the magnetic field, without impacting too much on the torus curvature. As described in Supporting Information, 32 Peltier cells were installed with an equal number of thermocouples and thermistors for temperature monitoring. The motherboard integrates all the AC/DC modules to power the cells and the read-out electronics, and includes a commercial FPGA with embedded ARM A9 microprocessor. The FPGA interfaces all the microprogrammed components on the motherboard and probes the hardware using ad-hoc Linux drivers and a mainline Kernel (Figure 2c). The Peltier cells are installed on the inner wall of the torus (16), as well as on the outer wall (16), plus 16 thermistors to measure wall temperature and 16 thermocouples to measure fluid temperature (Figure 2d). When the Peltier cells are steadily switched on, heat is brought to the inner wall and removed from the outer one (Figure 2e and 2f).

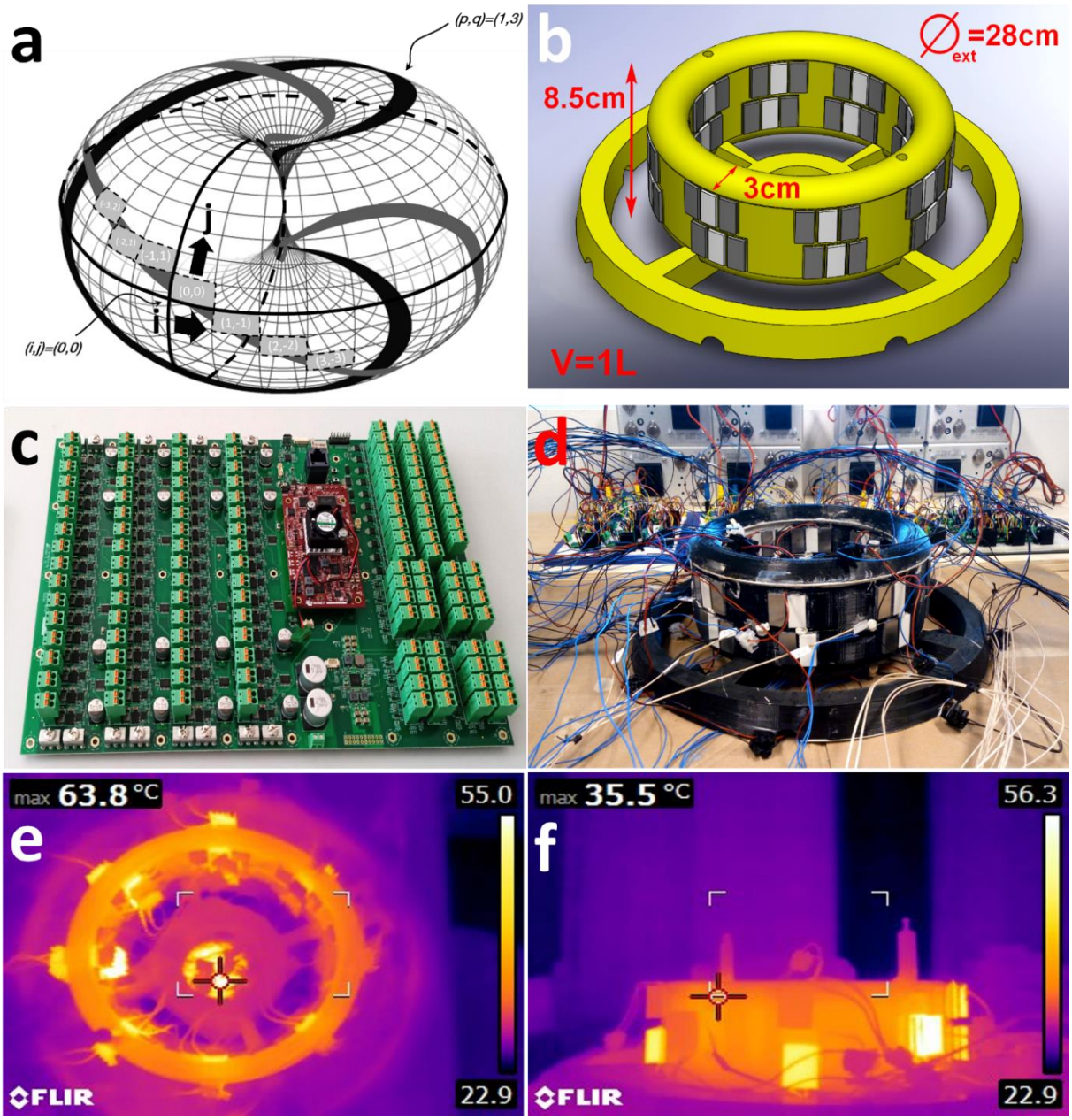

Figure 2: TORODYNA system. a) torus surface coordinate system with two Hopfions shown. b) 3D rendering of the prototype. c) Peltier Array Controller (PAC) based on a custom design. d) overview of the TORODYNA fully connected to powering/measurement devices. e) top view with thermal camera. f) side view with thermal camera.

Ferrofluid injection

Considering the smaller surface area of the inner wall and the lack of optimal airflow inside the torus, it has been found more efficient to heat the latter while cooling down the external one. Around the TORODYNA three separate coils are wound: one coil is used to extract energy and monitored via impedance measurements and it has two possible configurations: a purely poloidal one (Figure 3c) and a mixed poloidal/toroidal configuration (Figure 3f) that were tested to verify the travelling density waves-induced electromotive force. The specific choice is as follows: supposing that the FF motion inside the torus has a purely toroidal component, then all of its magnetic flux can be optimally intercepted by purely poloidal coils. If, on the other case, the FF motion inside the torus is helical (hence the velocity field has a toroidal component plus a poloidal one), then its magnetic flux can be optimally intercepted by mixed poloidal/toroidal coils. Other two coils (one poloidal and one toroidal) are used to induce a magneto-static field that helps in the initial phase to obtain a net clockwise flow along the toroidal coordinate. After a few minutes, both coils are disconnected to measure the pure harvesting component of electromotive force. The torus is filled with water and a small amount of FF (biphasic state). Injection of 1 mL of FF into water can be monitored as perturbation of the impedance of the system, the FF acting as a high permeability core of a discrete inductor (Figure 3a, b, d and e), and takes place at the time marked with α. It is possible to appreciate the increase of inductance of 45 nH with purely poloidal coil and of 65 nH with mixed poloidal/toroidal coil. The value of inductance with an empty tank is different in the two cases as the concatenated magnetic flux is directly proportional to the coil area times the number of windings squared (2,976.75 cm^2 in the former case and 6,037.5 cm^2 in the latter, same ratio of ~2 is kept in the measurements). The difference in the measured increase of inductance is the result of a more efficient concatenation

with complex fluid movements. The resistive part of impedance is used to monitor the energy output of the harvester, working on the equivalent circuit composed by the parallel between an ideal inductor (our extracting coil) and the impedance meter. What we read as a resistance variation, 800 μΩ for purely poloidal coil and 250 μΩ for mixed poloidal/toroidal coil, is due to the electromotive force generated in the experiment.

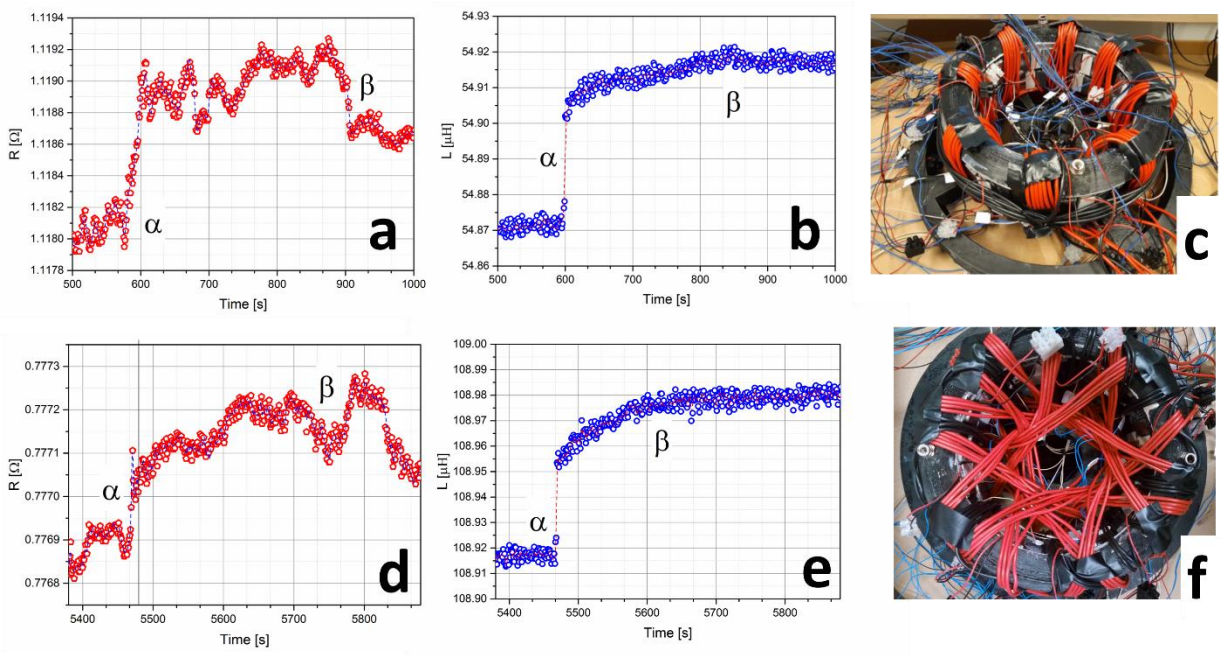

Figure 3: Effect of the injection of 1 mL FF in water. a) series resistance versus time of poloidal extraction coil. b) series inductance versus time of poloidal extraction coil. c) overview of poloidal coils. d) series resistance versus time of mixed toroidal/poloidal extraction coil. e) series inductance versus time of mixed toroidal/poloidal extraction coil. f) overview of mixed toroidal/poloidal coils.

Steady state functioning

A steady state characterization of the TORODYNA filled with 10 ml of FF in water lasts several hours (Figure 4a). The real ΔT submitted to the FF is 1.25 °C and is stable within 0.1 °C, while temperature uniformity can be evaluated by plotting all thermocouples responses (see Supporting Information); the Peltier cells have been switched on at t=0 (α) and after 1h the TORODYNA

reached dynamically stable operation (γ). In order to characterize also the thermalization back to room temperature, after 2h the system was switched off (δ) and switched on again (ε). Thermal fluctuations can be visualized plotting the difference between average temperature and any of the 16 sensors output data (Figure 4b), and Fourier analysis clearly shows how a fundamental mode is found with a period of about 150 s (*s* for single mode) and several other oscillation modes are present. Considering the winding periodicity (8 poloidal windings positioned every 10 cm) we can evidence the period corresponding to a packet of FF travelling across the whole toroidal axis (*t* for total mode, 360 °) and multiples of two (720°) and three (1080°) complete turns (Figure 4c). There is an excellent matching with impedance measurements, where monitoring of both the resistance and inductance component (Figure 4d, e) and consequent Fourier analysis evidences how all the most important spectral components (the fundamental *s*, the global *t* and the multiples at 720 and 1080°) are still present. Overall we could measure an electrical output of 10.4 μW/°C exploiting 10 mL of FF, in a situation where the Carnot efficiency between T_h=38.22 °C and T_c=37 °C is η=0.3918 %, with a thermal input power of 1.4 W giving a maximum theoretical output of 5.485 mW/°C. By filling up the reactor with only FF, we can already achieve 1.040 mW/°C or approximately 20% of the Carnot efficiency. For comparison, the best performance recorded in an oscillating heat pipe based on the oscillation of a bulk NdFeB permanent magnet of 3.17 mm diameter is 2.1 μW/W_{Th} against 9.3 μW/W_{Th} measured on our liquid-enabled technology with 10 mL of FF (therefore 930 μW/W_{Th} for a 1 L volume) [42]. We may compare the achieved efficiency with the two most efficient WHR systems for industrial applications, even if suitable for higher temperature range: Peris et al. [43] were able to reach a maximum gross electrical efficiency of 12.32 % by means of the application of an ORC to the waste heat coming from a ceramic factory (200-300 °C), which corresponds to 37% of the

Carnot efficiency; Wu et al. [44] proposed a novel type of CDTCC able to increase the net power output of gas turbines up to 26.3 % operating in the range of 250-500 °C, that is about 52% of Carnot efficiency. It should be noted, however, that such efficiencies were obtained at a much higher temperature and those heat recovery systems would not be able to work at the temperature used in our test, therefore the comparison done should be considered with particular care.

The system can operate continuously while the thermal gradient is kept across the tank width. The periodicity of both inductance and thermal waves is a consequence of the movement of density waves across solenoids, each amplitude peak corresponding to the transit of a packet in one of the extraction sections.

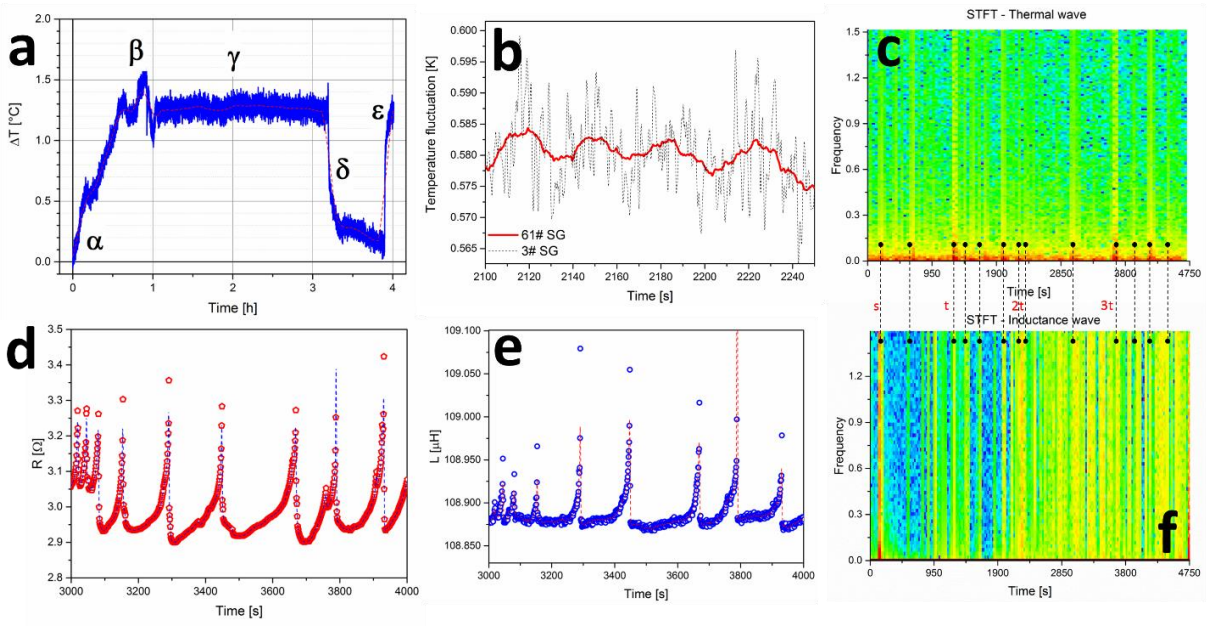

Figure 4: Steady-state operation. a) Effective ΔT on the fluid (dashed in red: Savitzky-Golay smoothing over 600 points). b) Thermal waves measured in the fluid along a period of 2 min (dashed in black: Savitzky-Golay smoothing over 3 points, continuous in red: over 61 points. c) Thermal waves evidenced by Short Time Fourier Transform (STFT) where fundamental periods have been evidenced. d) Series resistance versus time showing oscillations in the steady state. e) Series inductance versus time showing oscillations in the steady state. f) Inductance fluctuations as evidenced by Short Time Fourier Transform (STFT).

Numerical analysis

A set of numerical simulations has been carried out to understand the main fluid dynamical phenomena occurring inside the vessel. The aim is to gain insight on how the flow develops inside the toroidal container as a consequence of the magnetization of the magnetic particles and the temperature difference between the walls. The opaqueness of the walls does not allow a visualization of the flow, nor it is possible, at this stage, to introduce velocimeters. Moreover, simulations allow to investigate if different positions of the permanent magnets would significantly alter the flow and, as a consequence, the electrical energy output.

Given the small size and large number of the suspended particles, the system is physically modelled as a two-phase system with an Eulerian-Eulerian approach, that is, both phases, the solvent and the suspended colloidal particles, are treated mathematically as interpenetrating continua. Moreover, by considering the small volume fraction of the solid phase, of the order of 10^{-2}, and the negligible inertia of the particles, particles are assumed to be in thermal equilibrium with the surrounding flow and the model is conveniently formulated in terms of the mixture velocity and temperature. The solid phase is described through its volume fraction φ. The small temperature differences, of the order of 1 °C, allow use of the Boussinesq approximation for natural convection, so that the mixture density $\rho(T, \varphi)$ is approximated as $\rho = \rho_0 + \rho_0[-\alpha(T - T_0) + (\xi - 1)(\varphi - \varphi_0)]$, where ρ_0 is the mixture density at the average temperature of the system T_0 and particle mean volume fraction φ_0 , α is the thermal expansion coefficient of the solution and $\xi = \rho_p / \rho_f$ is the ratio of the density of the particles to the density of the solution. Particles are subject to the hydrodynamic interaction with the solution, which includes the thermophoretic force, and to the magnetophoretic force due to the externally imposed magnetic

field. The magnetophoretic force per unit volume of the mixture can be expressed as $f_M = \varphi\mu_0{}^* M \nabla H$, where $\mu_0{}^*$ is the magnetic permeability of vacuum, H the modulus of the magnetic field and M the magnetization of the particles, which depends on the magnetic field and the temperature, and is expressed by a magnetic equation of state. Since temperature variations in the flow are small, we choose the following relation, $M = \chi H - K(T - T_0)$, where χ is the magnetic susceptibility and K the pyromagnetic coefficient. Therefore, the mixture continuity and momentum balace equation for the mixture in the Boussinesq approximation are as follows

$$\nabla \cdot u = 0 \quad (1)$$

$$\rho_0 \left(\frac{\partial u}{\partial t} + u \cdot \nabla u\right) = -\nabla P + \mu \nabla^2 u + f_b - \varphi_0 \mu_0 K (T - T_0) \nabla H \quad (2)$$

Where ρ_0 is the mixture density at the average temperature of the system T_0, **u** is the mixture velocity, t is time, μ is the dynamic viscosity of the suspension, $P = p - \mu^*{}_0 \chi H^2 / 2$

is the modified pressure, $\mathbf{f}_b$ is the buoyancy force, given by

$\mathbf{f}_b = \rho_0 [(\xi - 1)(\varphi - \varphi_0) - \alpha(T - T_0)] \mathbf{g}$, φ_0 is the particle mean volume fraction, K the pyromagnetic coefficient, and H the modulus of the magnetic field. Notice that only buoyancy and magnetic forces enter in the momentum equation for the mixture, because the thermophoretic force is an internal force between the fluid and suspended particles. The model includes the equation for the mixture temperature, that is,

$$\frac{\partial T}{\partial t} + \nabla \cdot (Tu) = \kappa \nabla^2 T \quad (3)$$

where κ is the thermal diffusivity, and the equation for the particle volume fraction. By neglecting particle inertia, the slip between particles and mixture is due to the forces acting on the particles, that is, Stokes drag, Brownian forces, thermophoretic and magnetophoretic forces, so that, including all these effects, the equation for the volume fraction φ becomes

$$\frac{\partial \varphi}{\partial t} + \nabla \cdot (\varphi u) = \frac{2}{9}\frac{R^2}{\nu}(1-\xi)\nabla\varphi \cdot g + \frac{2}{9}\frac{R^2}{\nu}\xi\nabla \cdot (\varphi M \nabla H) + \kappa_p \nabla^2 \varphi + \kappa_T \nabla \cdot (\varphi \nabla T) \quad (4)$$

Here R is the radius of the particles, $\nu = \mu/\rho_f$ the kinematic viscosity of the carrier fluid, and κ_p is the Fickian diffusion coefficient due to the brownian forces on the particles, given by the Nernst-Einstein relation $\kappa_p = k_B T/(6\pi\mu R)$ (k_B is the Boltzmann constant). The last term in equation (4) describes the particle flux induced by a temperature gradient, which produces a relative velocity between particles and solution equal to $-\kappa_T \nabla T$, where κ_T is the thermophoretic diffusion coefficient, which quantifies the strength of the colloidal thermophoresis. By assuming that the magnetization is much weaker than the externally imposed magnetic field, due to the low volume fraction of the suspended particles, $\boldsymbol{H}$ can be obtained by integrating the Maxwell equations in absence of magnetic induction, which leads to

$$H = \nabla\psi, \psi(x) = \frac{1}{4\pi}\int_{V_m} \frac{m(y)\cdot(x-y)}{|x-y|} dy_1 dy_2 dy_3 \quad (5)$$

where ψ is the magnetic potential, $\boldsymbol{x}$ the vertical coordinate, $\boldsymbol{y}$ the poloidal coordinate, m is the magnetization per unit volume of the external permanent magnets, and the integration is carried out on the volume V_m of the magnet(s). Due to the simplification of the equation for particle magnetization, the resulting model can be considered a simplified version of the model used by Suslov [45] in the part dealing with thermomagnetic convection.

By neglecting the confinement in the vertical direction, and considering only the flow in the core of the toroidal configuration, governing equations (1-2-3-4) are solved in a parallelepiped domain between two vertical walls. A scheme of the simplified flow domain is shown in figure 5(a), together with two of the investigated magnet configurations. In this way, the topmost and bottom most portions of the vessel, where the vertical convective flow changes direction, are excluded by the simulation, which considers only the central portion of the vertical extent of the system.

The resulting partial differential equations are discretized with a mixed spectral-finite difference scheme (following the lines of Passoni et al. [46]): a Fourier-spectral discretization has been used along both the vertical and toroidal coordinates while finite differences are used along the poloidal axis. No-slip boundary condition for the velocity field and Dirichlet boundary conditions are imposed on the two vertical walls, while periodic boundary conditions are used in the other directions. A fourth order standard Runge-Kutta method has been used for time integration.

The magnetic field is provided by a set of permanent magnets, located around the cell, arranged in vertical strips of opposite facing magnets (Figure 5a and 5d). They are simulated by considering them as infinite in the vertical direction so that the magnetization, computed by equation (5), is perpendicular to the TORODYNA walls.

Convection movements along the vertical axis are a direct consequence of the temperature gradients in the flow domain. Hotter volumes are associated to lower flux densities and the resulting motion is upwards near the warmer wall and downwards near the colder wall. Since the Rayleigh number is relatively small, the flow remains laminar, and the vertical component is

always the dominating one. The other two velocity components, normal to the wall, i.e. directed across the vessel thickness, and along the toroidal axis, are a direct consequence of thermomagnetic force, as buoyancy does not act in such directions. Therefore, the position of the magnets and the intensity of the magnetic field directly modulate these components of velocity, which is important for the creation of three-dimensional cells able to generate a flux of magnetized particles which can be intercepted by the coils. The simulations allow computation of the magnetic flux through an arbitrary surface, so that it is possible to understand where the extraction coils must be ideally located to increase energy extraction efficiency. It is clear that the asymmetry between upwards and downwards movements, induced by the magnetic field, brings a preferable configuration. In this regards, the main outcome is that, having purely poloidal coils, the configuration that maximizes the magnetic flux, and therefore the overall energy efficiency, corresponds to perfectly asymmetric magnets (i.e., shifted by half their pitch, see Figure 5d, with a total phase mismatch along the toroidal direction of the magnetic fields generated by the opposite facing magnets). Such a configuration is potentially able to increase the magnetic flux up to 80% with respect to the basic configuration with directly opposing

magnets. Therefore, the overall efficiency of the system could be further increased.

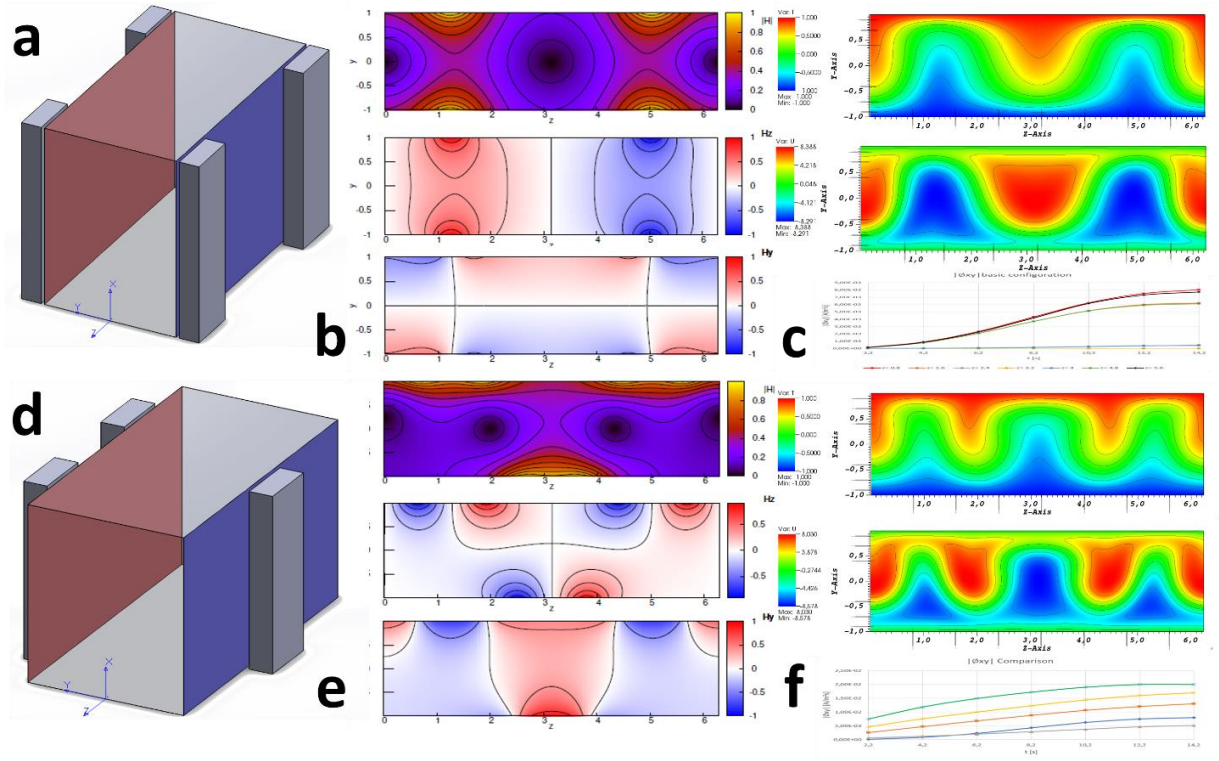

Figure 5: Steady-state operation. a) Simulation volume where the permanent magnets on the hot and cold wall are facing each other. b) Solution of Laplace equation for magnetic potential, from the top: magnetic field strength, toroidal component of magnetic field, poloidal component of magnetic field. c) Solution of thermomagnetic advection equation, from the top: temperature, vertical component of velocity, toroidal component of magnetic flux. d) Optimized simulation volume where the permanent magnets on the hot and cold wall are asymmetric and shifted. e) Solution of Laplace equation for magnetic potential, from the top: magnetic field strength, toroidal component of magnetic field, poloidal component of magnetic field. f) Solution of thermomagnetic advection equation, from the top: temperature field, vertical component of velocity, toroidal component of magnetic flux.

Conclusions

A new family of devices conceived to impact the landscape of low enthalpy heat recovery, based on thermomagnetic hydrodynamic effects, was designed, realized and characterized. They use as input a thermal gradient and give as output electric energy, the active part being a

functional liquid. The prototype is made with low cost materials and technologies, in a responsible and sustainable manner, avoiding toxic/polluting elements. At this stage, additional refinement and improvements are needed, especially optimizing the geometry, heat transfer capability, configuration of magnetic field together with thermal gradient, and power extraction systems. Furthermore, the performances have been investigated by using a water-oil based FF mixture with a small amount of magnetic nanoparticles able to induce the electromotive force and generate power from the waste heat. For all of these reasons, TORODYNA is not here presented as breakthrough in competition with already existing WHR systems which are, by contrast, optimized in the design, tested in a relevant environment, commercialized and employed in a broad range of industries and domestic plants, but rather as the first, promising, experimental result that could profitably be scaled up (or down) and provide a new solution for low enthalpy WHP applications.

So far, the efficiency reached in converting a tiny thermal gradient (1.25 °C) into electrical energy is 20% of the corresponding Carnot efficiency, representing therefore an important milestone in the research panorama, but also leaving room for future improvements, which are already in progress. Sources of losses are here summarized, providing the directions of improvement of our future research:

1) we are not able to concatenate the entire magnetic flux, as highlighted by numerical simulations; an optimal choice for the positioning of magnets, coils and fluid velocity vector could significantly increase the conversion efficiency;

2) the biphasic nature of our experiments, where FF is injected into water, provides a sub-optimal positioning of FF packets with respect to hot/cold zones;

3) partial sedimentation of FF nanoparticles due to interaction with water, with a concurrent reduction of the amount of matter able to induce an electromotive force in the extraction coils.

4) the liquid has a finite viscosity, therefore part of the work produced by the thermal gradient is absorbed to keep it moving;

Besides these losses, we suggest several improvements that can increase the power conversion:

1) the reduction of the thermal losses would allow to transfer a higher fraction of the available temperature difference to the fluid, increasing the temperature gradient which drives the flow;

2) an increased saturation magnetization of the FF would induce higher electromotive forces on the extraction coils;

3) smaller section wires would allow to position the coils closer to the device and to increase the number of windings, thus increasing the energy extracted.

The performance achieved is 442 times higher than the most similar technology available nowadays, known as oscillating heat pipe where, conversely to TORODYNA, the device is based on the phase transition of a non-magnetic solvent of their FF.

Supporting Information.

Includes: methods, design.

Acknowledgements

The Authors wish to thank: Politronica Inkjet Printing S.r.l. for providing the 3d printed prototype of the TORODYNA vessel for free; Dr. Claudio Lorini for the design and tutoring done on the PAC custom circuit; Prof. Pirri as Coordinator of the CSFT center of IIT.

References

[1] Jun'ya Takakura, Shinichiro Fujimori, Naota Hanasaki, Tomoko Hasegawa, Yukiko Hirabayashi, Yasushi Honda, Toshichika Iizumi, Naoko Kumano, Chan Park, Zhihong Shen, Kiyoshi Takahashi, Makoto Tamura, Masahiro Tanoue, Koujiro Tsuchida, Hiromune Yokoki, Qian Zhou, Taikan Oki and Yasuaki Hijioka, "Dependence of economic impacts of climate change on anthropogenically directed pathways", *Nature Climate Change* **9** (10), 737-741, 2019, doi: 10.1038/s41558-019-0578-6;

[2] Vaclav Smil, "Energy Transitions - History, Requirements, Prospects", 1st Edition, ABC-CLIO, 2010, ISBN: 0313381771, 9780313381775;

[3] Bo Liu and Deepak Rajagopal, "Life-cycle energy and climate benefits of energy recovery from wastes and biomass residues in the United States", *Nature Energy* **4**, 700–708, 2019, doi: 10.1038/s41560-019-0430-2;

[4] Ilona Johnson, William T. Choate, Amber Davidson, "Waste Heat Recovery. Technology and Opportunities in U.S. Industry". United States: N. p., 2008, Web, doi: 10.2172/1218716;

[5] Laia Miró, Russell McKenna, Tobias Jäger, and Luisa F. Cabeza, "Estimating the industrial waste heat recovery potential based on CO2 emissions in the European non-metallic mineral industry", *Energy Efficiency* **11**, 427–443, 2018, doi: 10.1007/s12053-017-9575-7;

[6] Navneet Soin, "Chapter 10: Magnetic Nanoparticles - Piezoelectric Polymer Nanocomposites for Energy Harvesting", *Magnetic Nanostructured Materials*, Pages

295-322, Elsevier, 2018, ISBN: 978-0-12-813904-2;

[7] Erik Garofalo, Luca Cecchini, Matteo Bevione, Fabio Mattiussi and Alessandro Chiolerio, "Waste Heat to Power: Technologies, Current Applications and Future Potentials." Unpublished results, submitted to Energy Technology;

[8] Joeri Rogelj, David L. McCollum and Keywan Riahi, "The UN's 'Sustainable Energy for All' initiative is compatible with a warming limit of 2 °C", *Nature Climate Change* **3**, 545–551, 2013, doi:10.1038/nclimate1806;

[9] Willem Jansen, Arnold M. Heitmann, Masanori Hanawa, "Recovery of automobile engine exhaust energy", *Proceedings of ASME Turbo Expo 2008: Power for Land, Sea and Air*, GT2008-50801, 733-739, Berlin, Germany, 2008, doi: 10.1115/GT2008-50801;

[10] Janie Ling-Chin, Huashan Bao, Zhiwei Ma, Wendy Taylor and Anthony P. Roskilly, W. T., Paul, A., "State-of-the-Art Technologies on Low-Grade Heat Recovery and Utilization in Industry", *Energy Conversion – Current Technologies and Future Trends thermal* **1**, 56-74, 2018, doi: 10.5772/intechopen.78701;

[11] Ruzhu Wang and Rogerio Oliveira, "Adsorption refrigeration—An efficient way to make good use of waste heat and solar energy", *Progress in Energy and Combustion Science* **32** (4), 424–458, 2006, doi: 10.1016/j.pecs.2006.01.002;

[12] Jun Mao, Zihang Liu, Jiawei Zhou, Hangtian Zhu, Qian Zhang, Gang Chen and Zhifeng Ren, "Advances in thermoelectrics", *Advances in Physics* **67** (2), 69–147, 2018, doi: 10.1080/00018732.2018.1551715;

[13] Anke Weidenkaff, "Better half found", *Nature Energy* **2**, 17010, (2017), doi: 10.1038/nenergy.2017.10;

[14] David C. Walther, Jeongmin Ahn, "Advances and challenges in the development of power-generation systems at small scales", *Progress in Energy and Combustion Science* **37** (5), 583-610, 2011, doi: 10.1016/j.pecs.2010.12.002;

[15] Steven A. Wright, Chal S. Davidson, William O. Scammell, "Thermo-economic analysis of four sCO2 waste heat recovery power systems", *5th International Symposium – Supercrit CO2 Power Cycles*, 1-16, San Antonio, Texas, 2016;

[16] Seijiro Sano, Hiroyuki Mizukami, Hiromasa Kaibe, "Development of High-Efficiency Thermoelectric Power Generation System", *Komatsu technical report* **49** (152), 2003.

[17] Kamran Zeb, Sahibzada M. Ali, Bilal Khan, Chaudhry A. Mehmood, N. K. Tareen, Waqar Ud Din, Umar Farid, U. and Ahun Haider, "A survey on waste heat recovery: Electric power generation and potential prospects within Pakistan", *Renewable and Sustainable Energy Reviews* **75**, 1142-1155, 2017, doi: 10.1016/j.rser.2016.11.096**;**

[18] Kasra Mohammadi and Jon McGowan, "Thermoeconomic analysis of multi-stage recuperative Brayton cycles: Part II – Waste energy recovery using CO2 and organic Rankine power cycles", *Energy Conversion and Management* **185**, 920–934, 2019, doi: 10.1016/j.enconman.2019.01.091;

[19] Sirko Ogrisek, "Integration of Kalina cycle in a combined heat and power plant,

a case study", *Applied Thermal Engineering* **29** (14-15), 2843–2848, 2009, doi: 10.1016/j.applthermaleng.2009.02.006;

[20] T. Yamashita, Y. Shimoyama, Y. Haga, T. D. Matsuda, E. Yamamoto, Y. Onuki, H. Sumiyoshi, S. Fujimoto, A. Levchenko, T. Shibauchi and Y. Matsuda, "Colossal thermomagnetic response in the exotic superconductor URu_2Si_2", *Nature Physics Letters* **11**, 17-20, 2015, doi: 10.1038/nphys3170;

[21] Tian Li, Xin Zhang, Steven D. Lacey, Ruiyu Mi, Xinpeng Zhao, Feng Jiang, Jianwei Song, Zhongqi Liu, Guang Chen, Jiaqi Dai, Yonggang Yao, Siddhartha Das, Ronggui Yang, Robert M. Briber and Liangbing Hu, "Cellulose ionic conductors with high differential thermal voltage for low-grade heat harvesting", *Nature Materials* **18**, 608–613, 2019, doi: 10.1038/s41563-019-0315-6;

[22] Mohammad Rahimi, Anthony P. Straub, Fang Zhang, Xiuping Zhu, Menachem Elimelech, Christopher A. Gorski and Bruce E. Logan, "Emerging electrochemical and membrane-based systems to convert low-grade heat to electricity", *Energy & Environmental Science* **11** (2), 276-285, 2018, doi: 10.1039/c7ee03026f;

[23] Liqiu Wang and Jing Fan, "Nanofluids Research: Key Issues," *Nanoscale Res. Lett.* **5**, 1241–1252, 2010, doi: 10.1007/s11671-010-9638-6;

[24] Alessandro Chiolerio and Marco B Quadrelli, "Colloidal Energetic Systems", *Energy Technology* **7** (5), 1800580, 2019, doi: 10.1002/ente.201800580;

[25] N. S. Susan Mousavi and Sunil Kumar, "Effective heat capacity of ferrofluids e Analytical approach," *International Journal of Thermal Sciences* **84**, 267-274, 2014,

doi: 10.1016/j.ijthermalsci.2014.05.012;

[26] Mengfei Yang, Robert O'Handley and Zhao Fang, "Modeling of Ferrofluid Passive Cooling System," *Proceedings of the COMSOL Conference*, Boston, Massachusetts, 2010;

[27] Stefan Odenbach, "Microgravity research as a tool for the investigation of effects in Magnetics", *Journal of Magnetism and Magnetic Materials* **201** (1-3), 149-154, 1999, doi: 10.1016/S0304-8853(99)00033-5;

[28] Kambiz Jahani, Maziar Mohammadi, Mohammad B. Shafii and Zahra Shiee, "Promising Technology for Electronic Cooling: Nanofluidic Micro Pulsating Heat Pipes", *Journal of Electronic Packaging* **135** (2), 2013, doi: 10.1115/1.4023847;

[29] Bruce Yellin, "Saving the future of Moore's law", *DELL Technologies white paper*, found at: *https://education.dellemc.com/content/dam/dell-emc/documents/en-us/2019KS_Yellin-Saving_The_Future_of_Moores_Law.pdf*, in March 2019;

[30] Sung Hwan Kim, "Germanium-source tunnel field effect transistors for ultra-low power digital logic", *PhD thesis*, UCB/EECS-2012-87, UC Berkley, 2012;

[31] Yimin Xuan and Wenlei Lian, "Electronic cooling using an automatic energy transport device based on thermomagnetic effect", *Applied Thermal Engineering* **31** (8-9), 1487-1494, 2011, doi: 10.1016/j.applthermaleng.2011.01.033;

[32] J. Gabriel Monroe, Erick S. Vasquez, Zachary S. Aspin, John D. Fairley, Keisha B. Walters, Matthew J. Berg, and Scott M. Thompson, "Energy harvesting via

ferrofluidic induction", *Proc. SPIE 9493, Energy Harvesting and Storage: Materials, Devices, and Applications VI*, 94930G, Baltimore, Maryland, 2015, doi: 10.1117/12.2178419;

[33] J. Gabriel Monroe, Erick S. Vasquez, Zachary S. Aspin, Keisha B. Walters, Matthew J. Berg, and Scott M. Thompson, "Electromagnetic induction by ferrofluid in an oscillating heat pipe", *Applied Physics Letters* **106**, 263901, 2015, doi: 10.1063/1.4923400;

[34] J. Gabriel Monroe, Swati Kumari, John D. Fairley, Keisha B. Walters, Matthew J. Berg, and Scott M. Thompson, "On the energy harvesting and heat transfer ability of a ferro-nanofluid oscillating heat pipe", *International Journal of Heat and Mass Transfer* **132**, 162-171, 2019, doi: 10.1016/j.ijheatmasstransfer.2018.11.096;

[35] Ravi Anant Kishore, Brent Davis, Jake Greathouse, Austin Hannon, David Kennedy, Alec Millar, Daniel Mittel, Amin Nozariasbmarz, Min Gyu Kang, Han-Byul Kang, Mohan Sanghadasa and Shashank Priya, "Energy scavenging from ultra-low temperature gradients", *Energy & Environmental Science* **12** (3), 1008-1018, 2019, doi: 10.1039/C8EE03084G;

[36] Anja Waske, Daniel Dzekan, Kai Sellschopp, Dietmar Berger, Alexander Stork, Kornelius Nielsch and Sebastian Fähler, "Energy harvesting near room temperature using a thermomagnetic generator with a pretzel-like magnetic flux topology", *Nature Energy* **4**, 68-74, 2019, doi: 0.1038/s41560-018-0306-x;

[37] Anthony P. Straub, Ngai Yin Yip, Shihong Lin, Jongho Lee and Menachem

Elimelech, “Harvesting low-grade heat energy using thermo-osmotic vapour transport through nanoporous membranes”, *Nature Energy* **1**, 16090, 2016, doi: 10.1038/nenergy.2016.90;

[38] Ganhua Xie, Pei Li, Zhen Zhang, Kai Xiao, Xiang-Yu Kong, Liping Wen, and Lei Jiang, “Skin-Inspired Low-Grade Heat Energy Harvesting Using Directed Ionic Flow through Conical Nanochannels”, *Advanced Energy Materials* **8** (22), 1800459, 2018, doi: 10.1002/aenm.201800459;

[39] Lujun Zhou, Yimin Xuan, Qiang Li, Wenlei Lian, “A new miniaturized engine based on thermomagnetic effect of magnetic fluids”, *Front. Energy Power Eng. China* **3**, 160–166, 2009, doi: 10.1007/s11708-009-0018-9;

[40] Hisoshi Yamaguchi, A. Sumiji, Shigemitsu Shuchi, T. Yonemura, “Characteristics of thermo-magnetic driven motor using magnetic fluid”, *Journal of Magnetism and Magnetic Materials* **272–276**, 2362–2364, 2004, doi: 10.1016/j.jmmm.2003.12.970;

[41] Kimura, Masaomi and Kobayashi, Hiroyuki and Tsutsui, Izumi, “Hopf term, fractional spin and soliton operators in the O(3) non-linear sigma model”, *Nuclear Physics B* **527** (3), 624-642, 1998, doi: 10.1016/S0550-3213(98)00389-7;

[42] J. Gabriel Monroe, Omar T. Ibrahim, Scott M. Thompson and Nima Shamsaei, “Energy harvesting via fluidic agitation of a magnet within an oscillating heat pipe”, *Applied Thermal Engineering* **129**, 884-892, 2018, doi: 10.1016/j.applthermaleng.2017.10.076;

[43] Bernardo Peris, Joaquin Navarro-Esbrì, Francisco Molés and Adrian Mota-Babiloni, “Experimental study of an ORC (organic Rankine cycle) for low grade waste heat recovery in a ceramic industry”, *Energy* **85**, 534-542, **2015**, doi: 10.1016/j.energy.2015.03.065;

[44] Chuang Wu, Xiao-jiang Yan, Shun-sen Wang, Kun-lun Bai, Juan Di, Shang-fang Cheng and Jun Li, “System optimisation and performance analysis of CO2 transcritical power cycle for waste heat recovery”, *Energy* **100**, 391-400, 2016, doi: 10.1016/j.energy.2015.12.001;

[45] Sergey A. Suslov, “Thermomagnetic convection in a vertical layer of ferromagnetic fluid”, *Physics of Fluids* **20**, 084101, 2008, doi: 10.1063/1.2952596;

[46] Giuseppe Passoni, Giancarlo Alfonsi and Massimo Galbiati, “Analysis of hybrid algorithms for the Navier-Stokes equations with respect to hydrodynamic stability theory”, *Int. J. Numer. Meth. Fluids* **38** (11), 1069-1089, 2002, doi: 10.1002/fld.259.